JOURNAL OF MATERIALS SCIENCE 35 (2000) 5485–5492

Reaction of Si_3N_4 with 25%Cr-20%Ni austenitic stainless steel under nitrogen or argon atmosphere

T. SHIMOO, K. OKAMURA
Department of Metallurgy and Materials Science, College of Engineering, Osaka Prefecture University, 1-1, Gakuen-cho, Sakai, Osaka 599-8531, Japan

D. SHIBATA
Graduate Student, Osaka Prefecture University, 1-1, Gakuen-cho, Sakai, Osaka 599-8531, Japan

In relation to joining of silicon nitride ceramics to metal, an extensive experimental study of the reaction between Si_3N_4 and 25%Cr-20%Ni austenitic stainless steel was conducted. Reaction rates were determined by thermogravimetry (TG) and reaction products were examined by X-ray diffraction. Cr_2N, CrN, $Cr_3Ni_5Si_2$ and Fe_3Si were produced under a nitrogen atmosphere. Fe_5Si_3 and FeSi also were produced under an argon atmosphere. The reaction products were analyzed according to thermodynamic considerations. The incubation period was found in TG curves and it was much shorter under a nitrogen atmosphere than under an argon atmosphere. The rates at early stages and late stages of reaction were given by linear and parabolic rate laws, respectively. Possible reaction mechanisms were proposed based on the results of the TG analysis. © *2000 Kluwer Academic Publishers*

1. Introduction

Silicon nitride is an attractive structural ceramic for high-temperature service conditions because of its excellent thermal and mechanical properties. The inherent brittleness associated with silicon nitride ceramic limits its application as structural components. In addition, complex-shaped and large sized components are difficult to fabricate, owing to poor machinability. In some cases, however, utilization of such ceramics can be expanded by joining ceramics to metals [1–9]. Among several joining methods proposed, in particular, diffusion bonding is a relatively simple technique for joining ceramics to metals. A reaction layer is formed at the silicon nitride/metal interface during diffusion bonding, and grows further in high-temperature service of the joints. Excessive growth of the reaction layer results in chemical and mechanical degradation of the joint. Thus, examination of the reaction products and reaction mechanism between silicon nitride and metal can provide useful insight into ceramic/metal bonding. Furthermore, the compatibility between silicon nitride and metal also is of great significance when ceramics are employed in direct contact with metals at elevated temperatures. Austenitic stainless steels with excellent heat-resistance characteristics are promising as the bonding couple to silicon nitride ceramics. Si_3N_4 produces silicides and nitrides by reacting with iron, chromium and nickel as the constituents of stainless steel [10–12]. Although the reaction between Si_3N_4 and austenitic stainless steel has been studied, the reaction products formed at the interface of ceramic/metal bonds have not yet been made clear [13–15]. This is because the reaction between bulk samples is too sluggish to detect the reaction products in a limited time heating. Using the powder sample, therefore, can reduce markedly the time required to observe the occurrence of new phases at the interface between Si_3N_4 and metal [16–21]. Thus, from a short period of experiment, it is possible to predict the interfacial reactions, the coexisting phases and the solid-state diffusion in the ceramic/metal bond after long time service at higher temperature.

In this paper, using a powder sample, the interaction of Si_3N_4 with austenitic stainless steel SUS3010L, in particular the effect of atmosphere, temperature and time which are the important parameters of diffusion bonding, was investigated in detail. The reaction products were determined by X-ray diffraction and were submitted to thermodynamic consideration. Thermodynamic modelling is a useful tool in predicting the behavior of Si_3N_4/metal systems. Furthermore, based on kinematic analysis of thermogravimetric data, the probable reaction mechanism was proposed in order to appreciate the growth of the reaction layer contributing to the bond strength.

2. Experimental procedure

The starting materials were silicon nitride powder (Ube Industries Ltd., SN-E10, α fraction $\geqq$ 95%, purity

98.5%, mean particle size 0.2 μm) and stainless steel SUS310L powder (Kobe Steel Ltd, Fine Atmel SUS310L, 0.014%C-0.85%Si-0.15%Mn-19.93%Ni-24.25%Cr, mean particle size 12.5 μm). Two grams of Si_3N_4 powder and 2 g of SUS310L powder were thoroughly mixed in a silicon nitride mortar, and then the mixture was compacted into a tablet of 20 mm in diameter.

The thermobalance unit for thermogravimetry (TG) consisted of an automatic recording balance (sensitivity: 0.1 mg) and a silicon carbide resistance furnace. When the desired temperature was reached, either nitrogen or argon gas was flowed from the bottom of the furnace at a pressure of 1.01×10^5 Pa and a flow rate of 2.5×10^{-5} $m^3 \cdot s^{-1}$. The tablet specimen was placed in a magnesia crucible (26 mm in inner diameter and 35 mm in depth) suspended into the hot zone of the furnace (alumina reaction tube of 44 mm in inner diameter) with a platinum wire connected to the balance. The mass change was recorded automatically during each experiment. Upon completion of the measurement, the specimen was cooled rapidly by raising the crucible into the low-temperature zone of the furnace. The reaction products were analyzed by X-ray diffraction.

3. Results

3.1. TG curves

Fig. 1 shows TG curves for Si_3N_4/SUS310L mixture heated continuously from room-temperature to 1573 K under a nitrogen or an argon atmosphere. The mass change, $100 \times \Delta W / W_0$ is the ratio of the mass change determined by TG to the initial mass of the mixture. Under a nitrogen atmosphere, a mass gain occurred at 950–1270 K and it turned to a rapid mass loss above 1270 K. Under an argon atmosphere, only mass loss was observed. There was a gradual mass loss at 1150–1220 K and rapid mass loss above 1220 K.

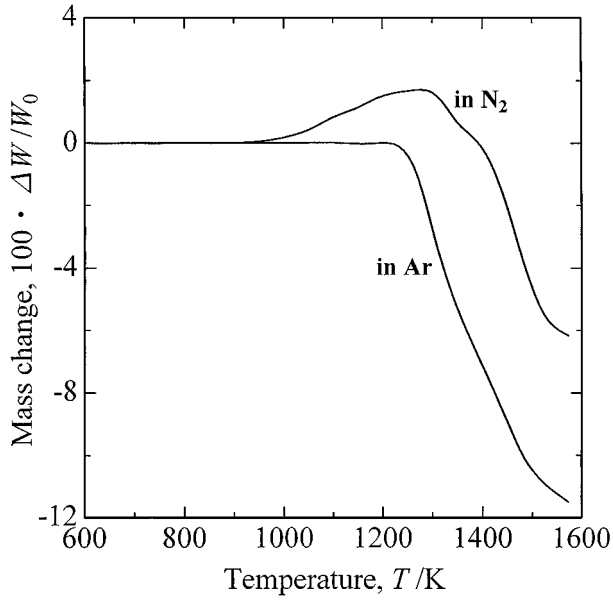

Figure 1 Mass change of Si_3N_4/SUS310L mixture heated continuously from room temperature to 1573 K.

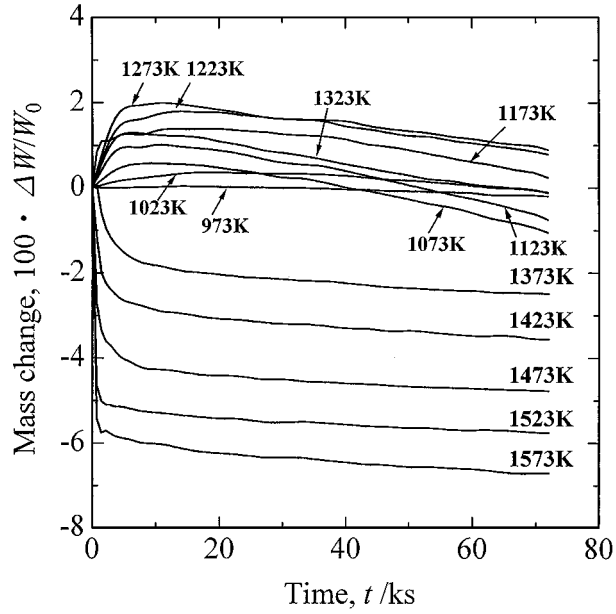

Figure 2 Mass change of Si_3N_4/SUS310L mixture heated isothermally at 973–1573 K under nitrogen atmosphere.

Fig. 2 shows TG curves for the Si_3N_4/SUS310L mixture heated isothermally at 973–1573 K under a nitrogen atmosphere. Below 1373 K, a mass gain was observed at the early stage of reaction. The mass gain turned to a mass loss during a long period of heating. The turning point from mass gain to mass loss was shortened with increasing temperature. Even above 1423 K, the mass increased rapidly at the extremely early stage of reaction, and subsequently, a remarkable decrease in mass within about 1 ks was followed by a gradual decrease in mass. As shown in Si_3N_4/Cr, Si_3N_4/Fe-Cr alloy and Si_3N_4/SUS304L steel systems, the mass gain is thought to be due to the nitridation of chromium as a constituent of SUS310L by nitrogen gas [16, 18, 20]. On the other hand, the mass loss is associated with the generation of nitrogen gas during formation of solid solution and silicides [16, 18, 20].

The isothermal TG curves under an argon atmosphere are shown in Fig. 3. No mass change was observed below 1073 K. The mass loss, which is attributable to the formation of solid solution and silicides [16, 18, 20], was observed above 1123 K. All TG curves were divided into three stages, as follows: first stage (the incubation period) at which the mass decreased only slightly; second stage at which the mass decreased rapidly within about 1 ks; and third stage at which the mass decreased gradually. The incubation period was remarkably shortened with an increase in temperature. Thus, the incubation period was only 120 s at 1573 K, while the incubation period appears to continue within the experimental time of 72 ks at 1073 K.

3.2. X-ray diffraction

Fig. 4 shows X-ray diffraction patterns of the Si_3N_4/SUS310L mixture heated for 72 ks at 973–1573 K under a nitrogen atmosphere. Cr_2N and CrN were produced below 1123 K and at 1073–1323 K, respectively

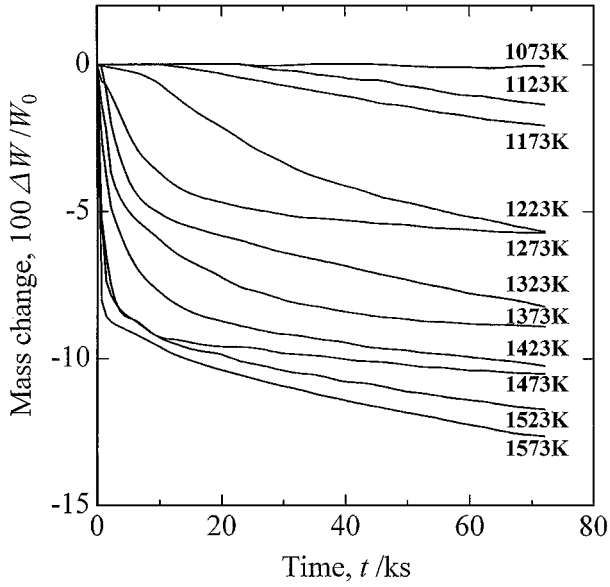

Figure 3 Mass change of Si_3N_4/SUS310L mixture heated isothermally at 1073–1573 K under argon atmosphere.

[22, 23]. The crystal structure of austenitic stainless steel SUS310L in the as-received state was identified as γ phase by X-ray diffraction [24]. Since a mass loss was observed in the TG curve, γ phase formed a solid solution with silicon even at 973 K. This was verified from the diffraction peaks of γ phase, which were shifted to the high angle side. While Si_3N_4 coexisted at all temperatures [25], γ phase disappeared at 1423 K and alternatively Fe_3Si was formed above 1373 K [26]. This suggests the formation of a reaction layer around the SUS310L particles. The diffraction pattern of an unknown phase (X) was observed at 1373–1523 K. From chemical analysis, X phase was estimated to be an Fe-Cr-Si-N quarternary compound [18]. In addition, $Cr_3Ni_5Si_2$ was formed at 1423–1523 K [27]. At 1573 K, both the compounds decomposed and only Fe_3Si was observed.

Fig. 5 shows X-ray diffraction patterns of the Si_3N_4/SUS310L mixture heated for 72 ks at 1073–1573 K under an argon atmosphere. At 1173–1323 K, Cr_2N was produced by the reaction of chromium in SUS310L with the free nitrogen from Si_3N_4. The diffraction patterns of Si_3N_4 were observed at all temperatures. It is evident from Fig. 3 that a solid solution of γ phase with silicon was formed above 1123 K. At 1223 K, the disappearance of γ phase and the alternative occurrence of Fe_3Si and $Cr_3Ni_5Si_2$ were observed. Above 1323 K, only iron silicides were detected owing to the decomposition of $Cr_3Ni_5Si_2$. With increasing temperature, the silicides were changed from Fe_5Si_3 at 1323 K to FeSi at 1523 K [28, 29]. Chromium and nickel as the constituents of γ phase (SUS310L) seem to be dissolved in the iron silicides. Therefore, strictly speaking, the silicides must be described as $(Fe,Cr,Ni)_3Si$, $(Fe,Cr,Ni)_5Si_3$ and (Fe,Cr,Ni)Si.

To reveal the temperature and time dependence of reaction products, Si_3N_4/SUS310L mixtures heated for 0.9, 7.2, 18 and 72 ks at temperatures from 973 to 1573 K were examined by X-ray diffraction. These results are summarized in Figs 6 and 7 by the temperature versus time diagrams for the reaction products. With increasing temperature and on prolonged heating, the reaction products under a nitrogen atmosphere changed from γ phase (Fe-Cr-Ni-Si solid solution) to Fe_3Si. Cr_2N and CrN were stable phases at lower temperatures. X phase (Fe-Cr-Si-N compound) and $Cr_3Ni_5Si_2$ were formed as transient products. On the other hand, the reaction products under an argon atmosphere (Fig. 7) changed from γ phase to FeSi, and then the Si/Fe ratio of silicides became larger in the following order: Fe_3Si, Fe_5Si_3, FeSi. In addition to the silicides, Cr_2N and $Cr_3Ni_5Si_2$ were transiently produced.

4. Discussion

4.1. Reaction products under a nitrogen atmosphere

Stainless steel SUS310L, which consists principally of iron, chromium and nickel, has an austenitic structure (γ phase). Since chromium increases the solubility of nitrogen in γ-Fe, the stainless steel has appreciable solid solubility of nitrogen [30]. In addition, chromium

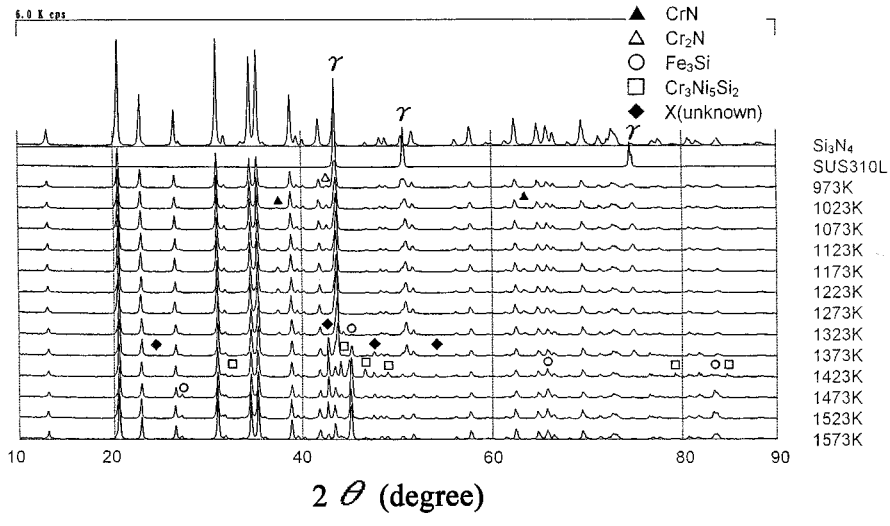

Figure 4 X-ray diffraction patterns of Si_3N_4/SUS310L mixture heated for 72 ks at 973–1573 K under nitrogen atmosphere.

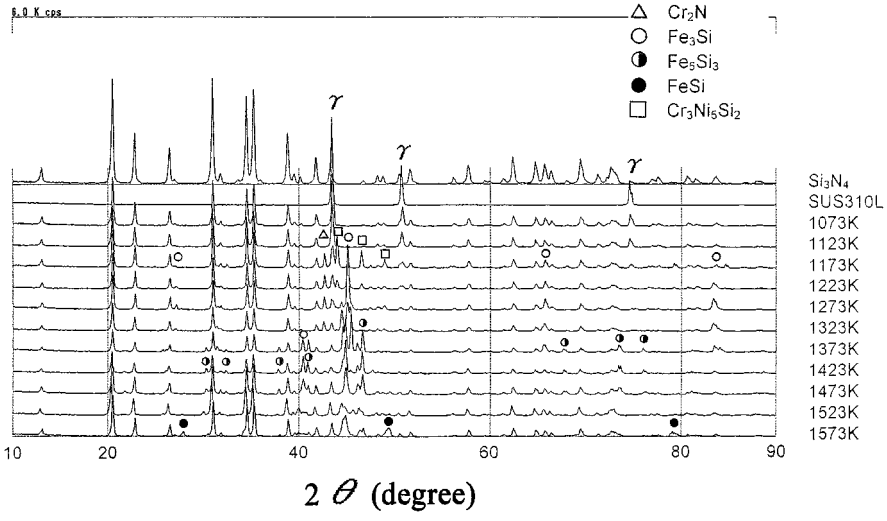

Figure 5 X-ray diffraction patterns of Si_3N_4/SUS310L mixture heated for 72 ks at 1073–1573 K under argon atmosphere.

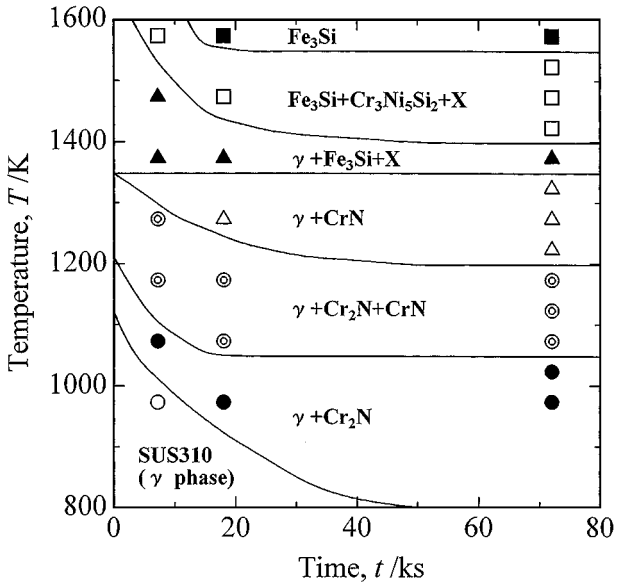

Figure 6 Temperature versus time relationship for reaction products in Si_3N_4/SUS310L mixture heated under nitrogen atmosphere.

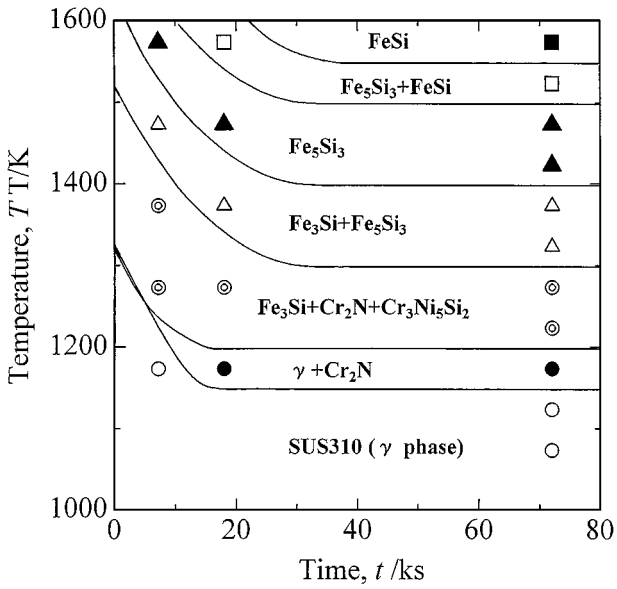

Figure 7 Temperature versus time relationship for reaction products in Si_3N_4/SUS310L mixture heated under argon atmosphere.

is a strong nitride-forming element. As seen from Fig. 2, mass gain occurred at early stages of reaction as a result of the interstitial solution of nitrogen in γ phase and the formation of chromium nitrides. Two types of nitride, Cr_2N and CrN, were produced by the reaction between chromium in SUS310L and nitrogen gas. Their standard free energy changes, ΔG°, are as given below [31]:

$$2\underline{\mathrm{Cr}} + 1/2\mathrm{N_2(g)} = \mathrm{Cr_2N(s)} \quad (1)$$

$$\Delta G^\circ/\mathrm{J\cdot mol^{-1}} = -99200 + 46.99T$$

$$\underline{\mathrm{Cr}} + 1/2\mathrm{N_2(g)} = \mathrm{CrN(s)} \quad (2)$$

$$\Delta G^\circ/\mathrm{J\cdot mol^{-1}} = -113400 + 73.22T$$

where $\underline{\mathrm{Cr}}$ stands for chromium which is dissolved in SUS310L. The Raoultian activity of chromium, a_{Cr}, relative to pure solid chromium must be used for the thermodynamic calculations. Fe-Cr-Ni alloy (SUS310L) may be approximately regarded as an ideal solution [32, 33]. Therefore, a_{Cr} is nearly equal to the mole fraction of chromium, $N_{\mathrm{Cr}} = 0.27$. The dissociation pressure of chromium nitrides is shown in Fig. 8. Under a nitrogen pressure of $p_{\mathrm{N2}} = 1.01 \times 10^5$ Pa (1 atm), Cr_2N and CrN are stable below 1443 and 1348 K, respectively. Figs 4 and 6 show that Cr_2N was produced below 1273 K and CrN was produced at temperatures of 1173–1323 K. This result is consistent with the thermodynamic calculation.

As seen from Fig. 2, the mass gain changed to mass loss at later stages of reaction. In addition, X ray diffraction showed a small peak shift of γ phase to the high-angle side below 1323 K (Fig. 4). These results imply the occurrence of reaction that involves the generation of nitrogen gas and the substitutional solution of silicon having a small atomic radius in the γ phase [31]:

$$\mathrm{Si_3N_4(s)} = 3\underline{\mathrm{Si}} + 2\mathrm{N_2(g)} \quad (3)$$

$$\Delta G^\circ/\mathrm{J\cdot mol^{-1}} = 723800 - 315T$$

where $\underline{\mathrm{Si}}$ stands for silicon in solid solution with SUS310L. From Fig. 6, it can be seen that Fe_3Si was produced above 1373 K. The reaction and its standard

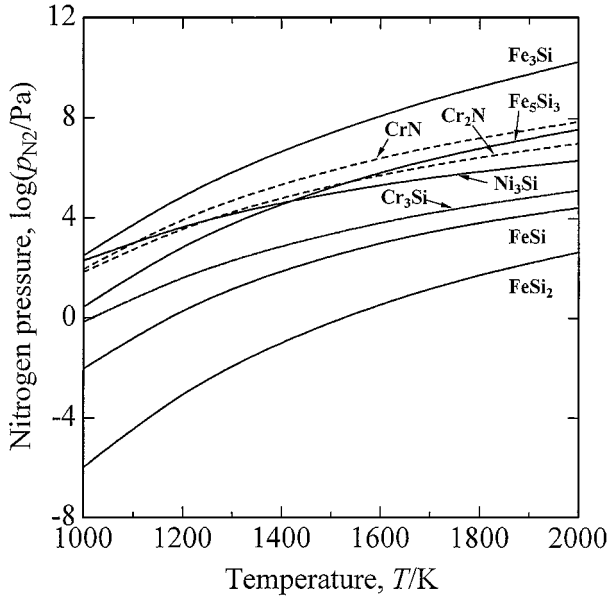

Figure 8 log p_{N2} versus temperature relationship for formation of Cr_2N, CrN, Fe_3Si, Fe_5Si_3, FeSi, $FeSi_2$, Cr_3Si and Ni_3Si.

free energy change for the formation of Fe_3Si are given by:

$$9\underline{Fe} + Si_3N_4(s) = 3Fe_3Si(s) + 2N_2(g) \quad (4)$$
$$\Delta G^\circ/J \cdot mol^{-1} = 479500 - 2.51T \ln T - 6.15 \times 10^{-2}T^2 - 6.40 \times 10^6 T^{-1} - 344T$$

Fe is iron as a constituent of SUS310L and its activity, a_{Fe}, is nearly equal to 0.54. Fe_5Si_3, FeSi and $FeSi_2$ also are found as iron silicides in the Fe-Si phase diagram [34]. A silicide with a high Si/Fe ratio is considered to be produced by reaction between Si_3N_4 and a silicide with a low Si/Fe ratio. Therefore, the following reaction should be considered:

$$15Fe_3Si(s) + 4Si_3N_4(s) = 9Fe_5Si_3(s) + 8N_2(g) \quad (5)$$
$$\Delta G^\circ/J \cdot mol^{-1} = 1749600 - 600T \ln T + 2.21 \times 10^{-1}T^2 + 2.87 \times 10^7 T^{-1} + 125T$$
$$3Fe_5Si_3(s) + 2Si_3N_4(s) = 15FeSi(s) + 4N_2(g) \quad (6)$$
$$\Delta G^\circ/J \cdot mol^{-1} = 1168000 - 0.88T \ln T + 8.80 \times 10^{-2}T^2 - 1.87 \times 10^6 T^{-1} - 709T$$
$$3FeSi(s) + Si_3N_4(s) = 3FeSi_2(s) + 2N_2(g) \quad (7)$$
$$\Delta G^\circ/J \cdot mol^{-1} = 697220 + 20.8T \ln T + 2.70 \times 10^{-3}T^2 - 5.10 \times 10^5 T^{-1} - 422T.$$

The values of ΔG° were calculated from the heat capacities, the standard enthalpies and entropies [35]. Fig. 8 shows temperature dependence of the equilibrium nitrogen pressures for the formation of the various iron silicides. Under a nitrogen atmosphere ($p_{N2} = 1.01 \times 10^5$ Pa), Fe_3Si, Fe_5Si_3, FeSi and $FeSi_2$ may be produced above 1214, 1468, 2330 and 2750 K, respectively. Thermodynamic calculation suggests that the reaction between Si_3N_4 and SUS310L produces both Fe_3Si and Fe_5Si_3 in the experimental temperature range. While Fe_3Si was produced above 1373 K, Fe_5Si_3 was not produced even at 1573K. X-ray diffraction did not detect Fe_5Si_3, probably due to the formation of a limited amount of Fe_5Si_3 as discussed below.

When all iron in SUS310L is converted into Fe_3Si, the mass loss, $-100 \times \Delta W/W_0$, is calculated to be 3.1 from the stoichiometry of reaction (4). The mass loss at 1423–1573 K exceeded 3.1 (Fig. 2), implying that other silicides also were produced. Thus, X-ray diffraction indicates the formation of X phase (Fe-Cr-Si-N quarternary compound) and $Cr_3Ni_5Si_2$ at 1423–1523 K. At 1573 K, however, only Fe_3Si was produced. This implies that both chromium and nickel formed the solid solution with Fe_3Si. According to the Fe-Si phase diagram, β_1 phase (Fe_3Si) is the nonstoichiometric compound which has the maximum solid solubility of 18.4mass%Si [34]. The maximum value of the mass loss, therefore, is calculated to be 6.1, when β_1 phase with 18.4mass%Si and the same Fe : Cr : Ni ratio as SUS310L is produced. This calculated value is smaller than the measured value of 6.7 at 1573 K. From thermodynamic estimation, this might be attributed to the formation of a small amount of Fe_5Si_3, which was not detected by X-ray diffraction.

The silicides of chromium and nickel, as the constituents of SUS 310L, also must be taken into consideration [31]. For there:

$$9\underline{Cr} + Si_3N_4(s) = Cr_3Si(s) + 2N_2(g) \quad (8)$$
$$\Delta G^\circ/J \cdot mol^{-1} = 405000 - 305T$$
$$9\underline{Ni} + Si_3N_4(s) = Ni_3Si(s) + 2N_2(g) \quad (9)$$
$$\Delta G^\circ/J \cdot mol^{-1} = 308900 - 329T.$$

The activities of chromium and nickel in SUS310L, a_{Cr} and a_{Ni}, are approximately 0.27 and 0.19, respectively. The equilibrium nitrogen pressures for the formation of Cr_3Si and Ni_3Si are shown in Fig. 8. Cr_3Si and Ni_3Si should be produced above 1956 and 1509 K under a nitrogen atmosphere ($p_{N2} = 1.01 \times 10^5$ Pa), respectively. Therefore, Ni_3Si should be produced at the experimental temperature. Ni_3Si, however, was not detected by X-ray diffraction, owing to the formation of a solid solution of nickel with Fe_3Si.

4.2. Reaction product under an argon atmosphere

Under an argon atmosphere, chromium is nitrided by the nitrogen gas liberated from Si_3N_4. The chromium nitrides, however, are unstable because of a low partial pressure of N_2 gas. Fig. 8 shows that the dissociation pressure of CrN is higher than that of Cr_2N. Therefore, only Cr_2N was produced at temperatures of 1173–1323 K (Figs 5 and 7). The coexisting phases were Fe-Cr-Ni-Si solid solution at 1173 K, and

$Fe_3Si + Cr_3Ni_5Si_2$ at 1223–1323 K. The observed mass loss implies that a part of the nitrogen gas evolved by the formation of such phases was consumed in producing Cr_2N. At higher temperatures, Fe_5Si_3 and FeSi were produced (at 1323 and 1523 K, respectively). The formation of iron silicides is represented by reactions (4), (5) and (6). Under an argon atmosphere, the partial pressure of nitrogen is considered to be low enough to produce Fe_5Si_3 and FeSi. For example, the thermodynamic calculation indicates that FeSi is produced under nitrogen pressure lower than 7.12×10^2 Pa at 1573 K. From Equations 8 and 9, the equilibrium pressures of Cr_3Si and Ni_3Si can be estimated as 4.86×10^3 and 1.67×10^5 Pa at 1573 K, respectively. Since these values are higher than the equilibrium nitrogen pressure for the formation of FeSi, both Cr_3Si and Ni_3Si should be produced under an argon atmosphere. However, they were not detected by X-ray diffraction. The reason is thought to be because both chromium and nickel form a solid solution with iron silicides, as confirmed by the following result. When the mass loss exceeds the stoichiometric value of 5.6 for $(Fe,Cr,Ni)_3Si$ and of 10.0 for $(Fe,Cr,Ni)_5Si_3$, $(Fe,Cr,Ni)_5Si_3$ and (Fe,Cr,Ni)Si should be produced, respectively. By comparing Fig. 7 with Fig. 3, it can be seen that the observed values agree roughly with the above stoichiometric ones.

4.3. Incubation period

As seen from Fig. 3, TG curves determined under an argon atmosphere are divided into three stages: a first stage where practically no reaction occurs, a second stage where the reaction proceeds rapidly and a third stage where the reaction gradually slows down its rate. The first stage is referred to as an incubation period. An incubation period was found in TG curves under a nitrogen atmosphere as well. Fig. 9 indicates the relationship between the incubation period and the reaction temperature for Si_3N_4/SUS310L. The TG curve at 1073 K under an argon atmosphere showed consistently the incubation period within the experimental time. The incubation period was shortened to about 147 s with increasing temperature. The duration of about 147 s is not the incubation period but is thought to be the heating time required to heat the sample to the given temperature. In addition, the incubation period is much shorter under a nitrogen atmosphere than under an argon atmosphere. This is because the chromium nitride layer is formed around SUS310L particles at the earliest stage of reaction under a nitrogen atmosphere. Si_3N_4 is difficult to react with SUS310L owing to different types of bond. Such a gap between Si_3N_4 and SUS310L phases is bridged by the formation of the chromium nitride with the common constituents of both phases, resulting in the earliest occurrence of the reaction between Si_3N_4 and SUS310L. Thus, the chromium nitride has a bridging effect on the reaction between Si_3N_4 and SUS310L. Consequently, under a nitrogen atmosphere the reaction between Si_3N_4 and SUS310L which caused the mass loss in TG curves was observed even at 973 K, whereas under an argon atmosphere, the reaction proceeded only above 1123 K.

4.4. Reaction mechanism

Fig. 2 indicates that it is very difficult to analyze kinematically the TG data under a nitrogen atmosphere. Therefore, only the rate data under an argon atmosphere (Fig. 3) is discussed.

In the early stage of reaction, Si_3N_4 reacts directly with SUS310L and nitrogen gas escapes through the interparticle pores in powders. In such a case, its rate is described by a linear rate law [17–21]:

$$100 \times \Delta W / W_0 = k_1 \times t \qquad (10)$$

where k_1 is a linear rate constant. Fig. 10 shows that the linear rate equation is applicable during the early stages of the TG curves. Arrhenius plots of the rate constant, k_1, are shown in Fig. 11. The variation of k_1 with temperature changes at 1423 K. Similar results were obtained for Si_3N_4/Fe, Si_3N_4/Fe-Ni alloy, Si_3N_4/SUS304L stainless steel and Si_3N_4/Ni-Cr alloy

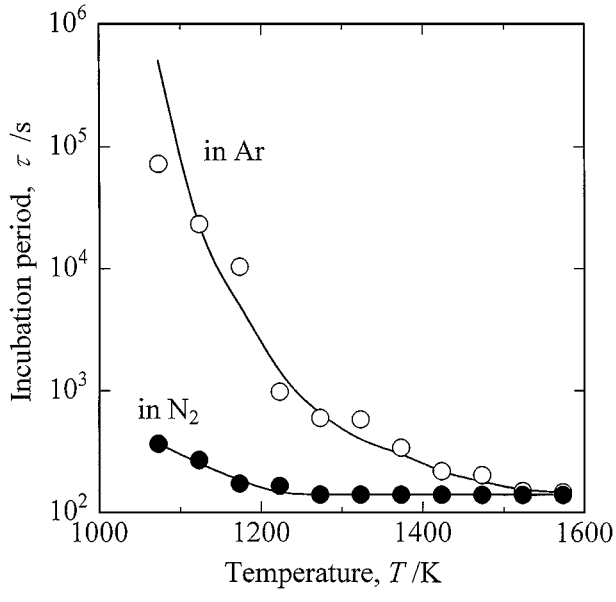

Figure 9 Incubation period for reaction between Si_3N_4 and SUS310L.

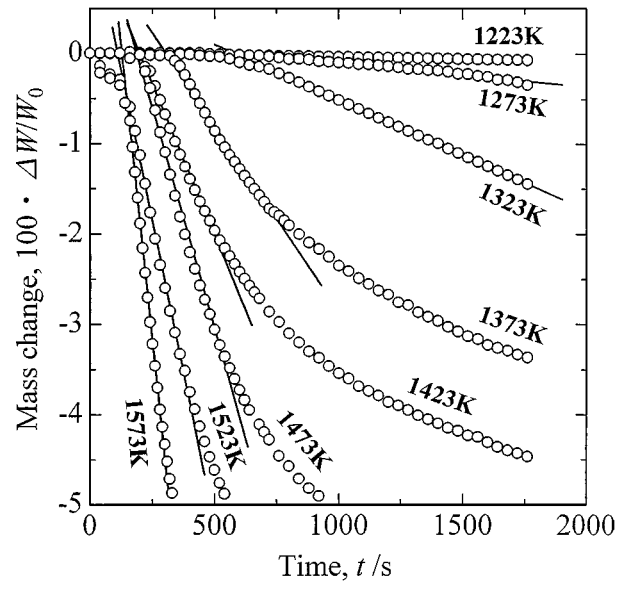

Figure 10 Application of linear rate law to TG data shown in Fig. 3.

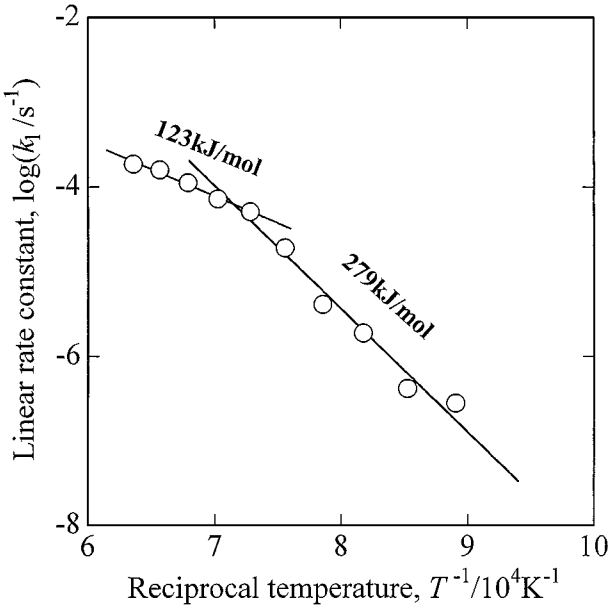

Figure 11 Arrhenius plots for rate constant of linear rate law, k_1.

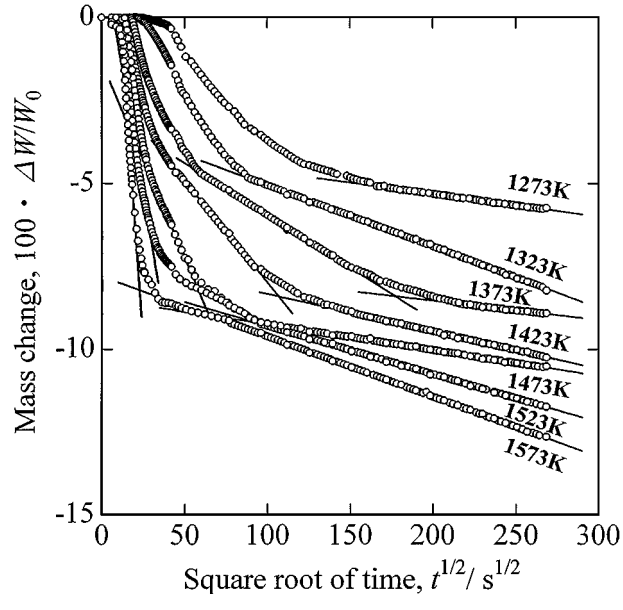

Figure 12 Application of parabolic rate law to TG data shown in Fig. 3.

systems [17–21]. The activation energies were estimated as 123 kJ/mol above 1373 K and 279 kJ/mol below 1373 K, respectively. The activation energy above 1373 K was nearly equal to that for Si_3N_4/Fe-Ni alloy, Si_3N_4/Fe and Si_3N_4/SUS304L systems above 1373 K; i.e., 98, 106 and 97 kJ/mol [17–20]. In addition, the values of k_1 varied within the same orders of magnitude: for example, 1.9×10^{-4} s^{-1} for Si_3N_4/SUS310L, 2.5×10^{-4} s^{-1} for Si_3N_4/Fe-Ni alloy, 3.9×10^{-4} s^{-1} for Si_3N_4/Fe and 2.6×10^{-4} s^{-1} for Si_3N_4/SUS304L at 1573 K. Therefore, the reaction rates of the four systems are considered to be determined by the same elementary step. The low activation energy is probably due to the weak temperature dependence of the diffusivity of gas (D); $D \propto T^{1.5}$ or $T^{1.8}$ [36]. At higher temperatures, the reaction proceeds rapidly to vigorously generate nitrogen gas, resulting in difficulty of nitrogen gas escaping through the interparticlar pores in the powder. Thus, the reaction rate at higher temperatures may be determined by gaseous diffusion. On the other hand, the activation energy for Si_3N_4/SUS310L system below 1373 K (279 kJ/mol) is double that above 1423 K (123 kJ/mol). Then, the rate constant, k_1, for Si_3N_4/SUS310L was smaller than k_1 for Si_3N_4/Fe, Si_3N_4/Fe-Ni alloy and Si_3N_4/SUS304L systems: for example, 4.2×10^{-7} s^{-1} for Si_3N_4/SUS310L, 1.1×10^{-6} s^{-1} for Si_3N_4/Fe-Ni alloy and 4.4×10^{-6} s^{-1} for Si_3N_4/Fe, 1.5×10^{-5} s^{-1} for Si_3N_4/SUS304L at 1173 K. The high activation energy and the small value of k_1 implies that the rate of the reaction between Si_3N_4 and SUS310L at lower temperatures is controlled by interfacial reaction.

When the metal particles were completely covered by a reaction layer, the reaction between Si_3N_4 and SUS310L proceeds through five basic steps:

1. Solid-state diffusion of Si through the reaction layer.
2. Solid-state diffusion of Fe, Ni and Cr through the reaction layer.
3. Chemical reaction at the interface between Si_3N_4 and reaction layer.
4. Chemical reaction at the interface between reaction layer and SUS310L.
5. Diffusion of N_2 gas through the interparticle pores.

The reaction rate between Si_3N_4 and metals was controlled by the solid-state diffusion through the reaction layer and consequently it obeyed the following parabolic rate law [17–21]:

$$100 \times \Delta W/W_0 = k_p^{1/2} \times t^{1/2} \qquad (11)$$

where k_p is a parabolic rate constant. Application of rate Equation 11 to the TG data under an argon atmosphere is shown in Fig. 12. The linear relations with different slopes were obtained in the ranges of $100 \times \Delta W/W_0 = -5 \sim -9$ and $\geqq -9$. Comparing Fig. 3 with Fig. 7 shows that each range approximately corresponds to the region of Fe_5Si_3 and FeSi, respectively. Neither the linear nor the parabolic rate law was applicable to the TG data in the range of $-2 \leqq 100 \times \Delta W/W_0 \leqq -5$. The reason is because the reaction rate is not controlled by a single elementary step. Fig. 13 shows Arrhenius plots of the parabolic rate constant, k_p. The slopes of plots yield the activation energies of 184kJ/mol in the Fe_3Si region and 494 kJ/mol in the Fe_5Si_3 region. Since iron is the main constituent of SUS310L, Fe-Si solid solution and iron silicides were mainly detected by X-ray diffraction. The estimated value in the Fe_3Si region is nearly identical to the activation energy of 209 kJ/mol for the interdiffusion of the Fe-Si system [37]. Compared to the value in the Fe_3Si region, the experimental value in the Fe_5Si_3 region is significantly larger. However, a discussion of this subject cannot be undertaken from the lack of information about the activation energy in the Fe_5Si_3 region.

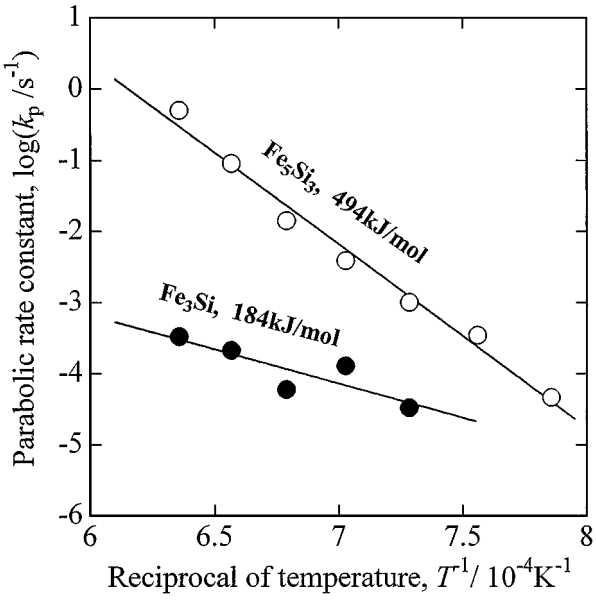

Figure 13 Arrhenius plots for rate constant of parabolic rate law, k_p.

5. Summary

Using mixed powder compacts, the products and mechanisms of reaction between Si_3N_4 and 25%Cr- 20%Ni austenitic stainless steel (SUS310L) have been investigated under a nitrogen or an argon atmosphere at temperatures from 973 to 1573 K.

Under a nitrogen atmosphere, the reaction of chromium in SUS304L with nitrogen gas yielded Cr_2N and CrN. During a long time heating, silicon was dissolved in γ-phase (SUS310L) as a solid solution by the solid-state reaction between Si_3N_4 and SUS310L. Above 1373 K, iron silicide, Fe_3Si was formed. In addition, an Fe-Cr-Si-N quaternary compound and $Cr_3Ni_5Si_2$ were formed at 1373 and 1423 K respectively, and then both compounds decomposed at 1573 K.

Under an argon atmosphere, Cr_2N was produced at temperatures between 1173 and 1373 K. A solid solution of γ-phase with silicon was formed at 1123 K, and alternatively, Fe_3Si and $Cr_3Ni_5Si_2$ occurred at 1223 K. While $Cr_3Ni_5Si_2$ decomposed at 1373 K, Fe_3Si was converted into FeSi through a transient Fe_5Si_3 phase at higher temperatures and on prolonged heating. Both chromium and nickel as the constituents of SUS310L are considered to form a solid solution with the iron silicides.

A very long incubation period was found in TG curves at lower temperatures under an argon atmosphere. The incubation period was shortened by a bridging effect of chromium nitride under a nitrogen atmosphere. The initial reaction rate under an argon atmosphere was described by a linear rate law, and the activation energy was 279 kJ/mol below 1373 K and 123 kJ/mol above 1423 K. The rate at late stages of reaction obeyed a parabolic rate law. The activation energies were 184 kJ/mol in the Fe_3Si region and 494 kJ/mol in the Fe_5Si_3 region.

Acknowledgement

This study was supported partly by a grant from the Tanikawa Fund for Promotion of Thermal Technology, which is gratefully acknowledged.

References

1. R. E. LOEHMAN and A. P. TOMSIA, *Am. Ceram. Soc. Bull.* **67** (1988) 375.
2. S. KANG, E. M. DUNN, J. H. SELVERIAN and H. J. KIM, *ibid.* **68** (1989) 1608.
3. G. ELSSNER and G. PETZOW, *ISIJ International* **30** (1990) 1011.
4. T. OKAMOTO, *ibid.* **30** (1990) 1033.
5. K. SUGANUMA, *ibid.* **30** (1990) 1046.
6. O. M. AKSELSEN, *J. Mater. Sci.* **27** (1992) 569.
7. *Idem., ibid.* **27** (1992) 1989.
8. J. M. HOWE, *International Mater. Rev.* **38** (1993) 233.
9. *Idem., ibid.* **38** (1993) 257.
10. F. WEITZER and J. C. SCHUSTER, *J. Solid State Chem.* **70** (1987) 178.
11. J. C. SCHUSTER, *J. Mater. Sci.* **23** (1988) 2792.
12. J. C. SCHUSTER, F. WEITZER, J. BAUER and H. NOWOTONY, *Mater. Sci. Eng.* **A105/106** (1988) 201.
13. M. J. BENNETT and M. R. HOULTON, *J. Mater. Sci.* **14** (1979) 184.
14. H. SUEYOSHI, M. TABATA, Y. NAKAMURA and R. TANAKA, *ibid.* **27** (1992) 1926.
15. B. T. J. STOOP and G. DEN OUDEN, *Met. Trans. A* **24A** (1993) 1935.
16. T. SHIMOO, Y. KOBAYASHI and K. OKAMURA, *J. Ceram. Soc. Jpn* **101** (1993) 675.
17. T. SHIMOO, T. YAMASAKI and K. OKAMURA, *J. Jpn Inst. Metals* **60** (1996) 72.
18. T. SHIMOO, D. SHIBATA, T. YAMASAKI and K. OKAMURA, *J. Ceram. Soc. Jpn* **105** (1997) 52.
19. T. SHIMOO, T. YAMASAKI and K. OKAMURA, *ibid.* **105** (1997) 734.
20. T. SHINOO, D. SHIBATA and K. OKAMURA, *ibid.* **106** (1998) 545.
21. T. SHIMOO, K. OKAMURA and M. ITOH, *J. Mater. Sci.* **33** (1998) 5169.
22. JCPDS 35-0803.
23. JCPDS 11-0065.
24. JCPDS 33-0397.
25. JCPDS 09-0250.
26. JCPDS 11-0616.
27. JCPDS 15-0793.
28. JCPDS 38-0438.
29. JCPDS 38-1397.
30. Y. IMAI, T. MASUMOTO and K. MAEDA, *J. Jpn Inst. Metals* **29** (1965) 866.
31. E. T. TURKDOGAN, "Physical Chemistry of High Temperature Technology" (Academic Press, New York, 1980) p. 5.
32. J. F. ELLIOTT, M. GLEISER and V. RAMAKRISHNA, "Thermochemistry for Steelmaking" (Addison-Wesley, Oxford, 1963) p. 503.
33. J. I. GOLDSTEIN, R. E. HANNEMAN and R. E. OGILVIE, *Trans. Met. Soc. AIME* **233** (1965) 812.
34. G. V. RAYNOR and V. G. RIVLIN, *Int. Met. Rev.* **30** (1985) 181.
35. G. V. SAMSONOV and I. M. VINIKII, "Refractory Compounds" (translated into Japanese) (Metallurgiya, Moscow, 1976) p. 141, 145, 162.
36. J. SZEKELY and N. J. THEMELIS, "Rate Phenomena in Process Metallurgy" (Wiley-Interscience, New York, 1971) p. 368.
37. H. MITANI, M. ONISHI and M. KAWAGUCHI, *J. Jpn Inst. Metals* **31** (1967) 1341.

Received 30 March 1999
and accepted 5 April 2000